Supplementary Materials

Lead-Free Organic Manganese (II) Bromide Hybrid with Highly Efficient and Stable Green Emission for UV Photodetection

Ye Tian [1], Qilin Wei [2,*], Lian Duan [3] and Chengyu Peng [3,*]

[1] School of Semiconductors and Physics, North University of China, Taiyuan 030051, China
[2] School of Chemistry and Chemical Engineering, Shandong University, Jinan 250100, China
[3] Traffic Information Engineering Institute, Guangxi Transport Vocational and Technical College, Nanning 530004, China
* Correspondence: qlwei@sdu.edu.cn (Q.W.); chengyu_peng@126.com (C.P.)

Experimental section

Materials, single crystal growth, and photodetector fabrication

Tetrabutylammonium bromide (TBABr, 99%), and Manganese (II) bromide tetrahydrate ($MnBr_2 \cdot 4H_2O$, 98 %) were purchased from Macklin, anhydrous ethanol (AR) was purchased from Guangdong Guanghua, and toluene (AR) was purchased from Chengdu Kelong.

Typically, 2 mmol TBABr and 1 mmol $MnBr_2 \cdot 4H_2O$ were fully dissolved in 2 mL anhydrous ethanol. Then, slowly add 3 mL toluene to the clear precursor solution. After 24 - 72 h, the green bulk single crystals can be obtained from the solution.

For preparing Ag/$(TBA)_2MnBr_4$/Ag photodetector, a thin layer of silver paste on the surface of $(TBA)_2MnBr_4$ single crystal, is then transferred to the oven to bake at 60 ℃ overnight. The distance of Ag electrodes was controlled to 5 mm. The detector uses 365 nm continuous laser as the excitation source. The distance between the light source and the detector is about 10 cm and the light source frequency is 8.22×10^{14} Hz.

Characterization

A SMARTLAB 3KW X-ray diffractometer with Cu Kα radiation (λ= 1.54059 Å) was used

to collect the powder X-ray diffraction data in the 2θ range of 5°- 50°. The scanning electron microscopy (SEM, Hitachi SU8020) was used to observe the morphology. The energy-dispersive spectrometry (EDS, Oxford X-Max Aztec) was used to collect the element composition and distribution. The Raman spectrum was characterized by WITec alpha300R Raman fluorescence spectrometer with a 633 nm laser as an excitation source. The photoluminescence (PL), PL excitation (PLE) spectrum, time-resolved photoluminescence (TRPL), photoluminescence quantum yields (PLQYs), temperature-dependent PL spectra, PLQY stability, and UV stability obtained on the Horiba Jobin Yvon Fluorolog-3 spectrometer and Zolix SFQY-9000 spectrometer. The Lambda 750 ultraviolet-visible spectrophotometer was used to measure the absorption spectrum. The thermal analysis was carried out on a Shimazu DTG - 60H instrument. The photoelectric properties of the as-fabricated LED device, including the emission spectra, correlated color temperature (CCT), and Commission Internationale de L'Eclairage (CIE) chromaticity coordinate were obtained on an ATA-1000 (Everfine, China) optoelectronic analyzer. A Keithley 2400 sourcemeter was used to collect the I-V curves of the Ag/$(TBA)_2MnBr_4$/Ag device.

Computational Details

The projector-augmented wave method is used to calculate the band structure, as implemented in the Vienna Ab initio simulation package (VASP). The generalized gradient approximation of the Perdew-burke-Ernzerhof parameterization is used for the exchange and correlation functional. The kinetic energy cutoff of 500 eV and a 4×4×4 Monkhorst-Pack k-mesh for the wavefunction basis set is used. The energy convergence criterion is set as 1.0×10^{-6} eV for structure relaxations.

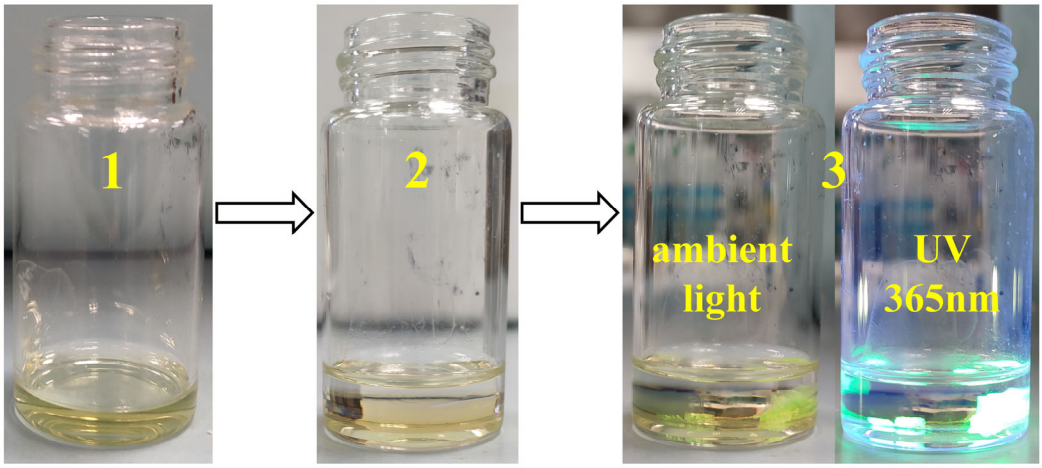

Figure S1. The photograph of the growth process of $(TBA)_2MnBr_4$ SCs.

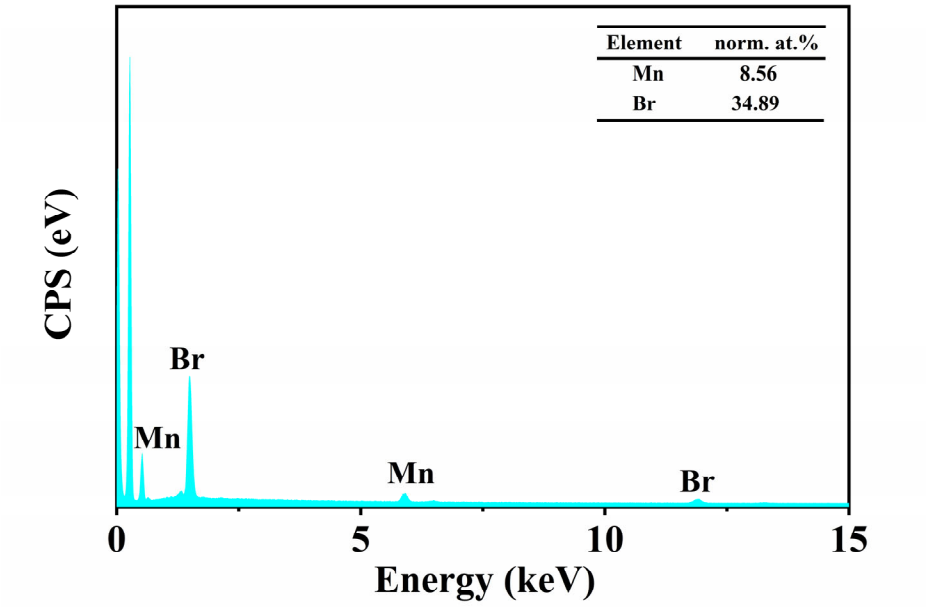

Figure S2. The Energy disperse spectrum of $(TBA)_2MnBr_4$.

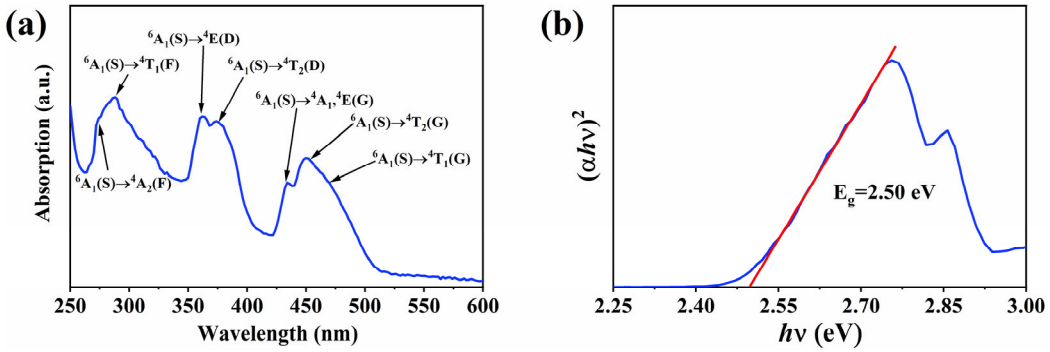

Figure S3. The UV-Vis absorption spectrum (**a**) of $(TBA)_2MnBr_4$ and corresponding Tauc plot (**b**).

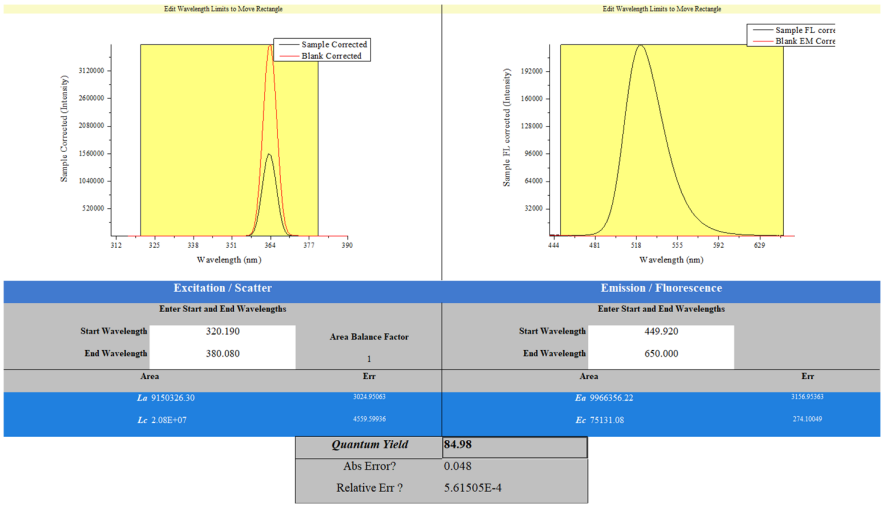

Figure S4. The PLQY measurement view of $(TBA)_2MnBr_4$ shows that the PLQY is as high as 84.98%. The excitation wavelength was 365 nm.

Table S1. Assignments of the observed Raman spectra of $(TBA)_2MnBr_4$ SCs.

Raman Wavenumber (cm^{-1})	Peak Assignment
80.43	$\delta[MnBr_4]^{2-}$
152.89	$\nu^{s}[MnBr_4]^{2-}$
253.59	$\nu^{as}[MnBr_4]^{2-}$
398.51	-
654.56	-
859.35	ρCH_2
906.96	ν(C-N)
1052.46	C-C
1124.93	-
1322.63	τCH_2
1398.16	$\delta^{s}CH_3$
1439.91	$\delta^{as}NH_3$
1464.47	δCH_2
1675.09	-
2865.09	$\nu^{s}CH_2$
2934.47	$\nu^{as}CH_2$

Where ν is stretching mode, δ is scissoring or bending mode, ρ is rocking mode, as is asymmetric mode, s is symmetric mode.

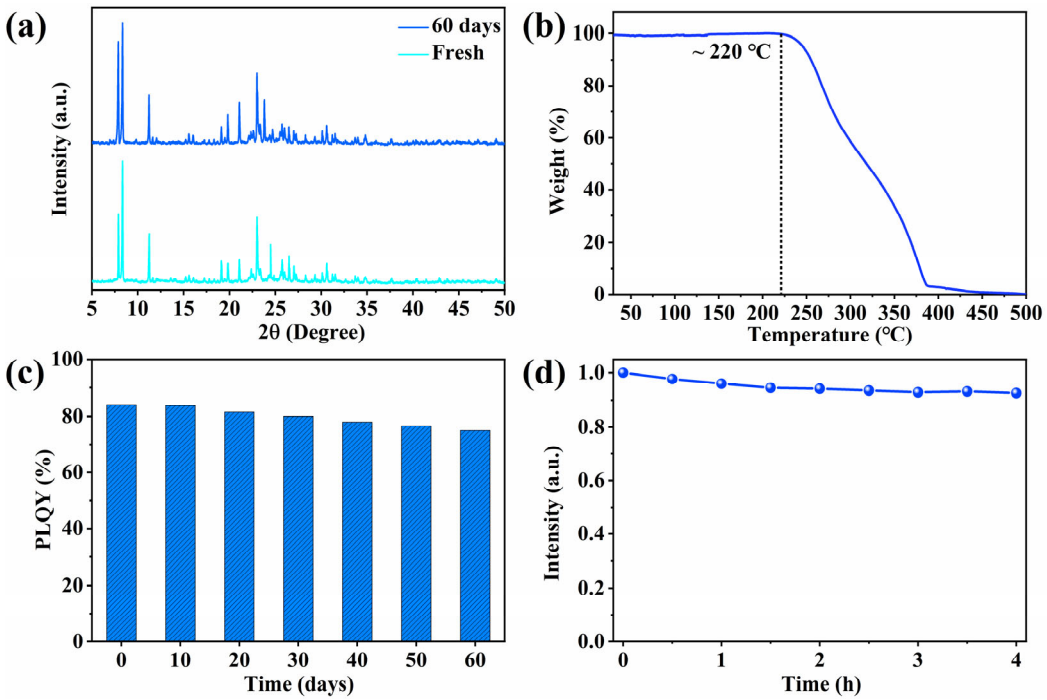

Figure S5. (**a**) The XRD patterns of $(TBA)_2MnBr_4$ before and after stored in ambient condition for 60 days. (**b**) TGA curve of $(TBA)_2MnBr_4$. (**c**) The PLQY value variation of $(TBA)_2MnBr_4$. (**d**) Long-term PL stability of $(TBA)_2MnBr_4$ under a 365 nm UV lamp within 4 h.

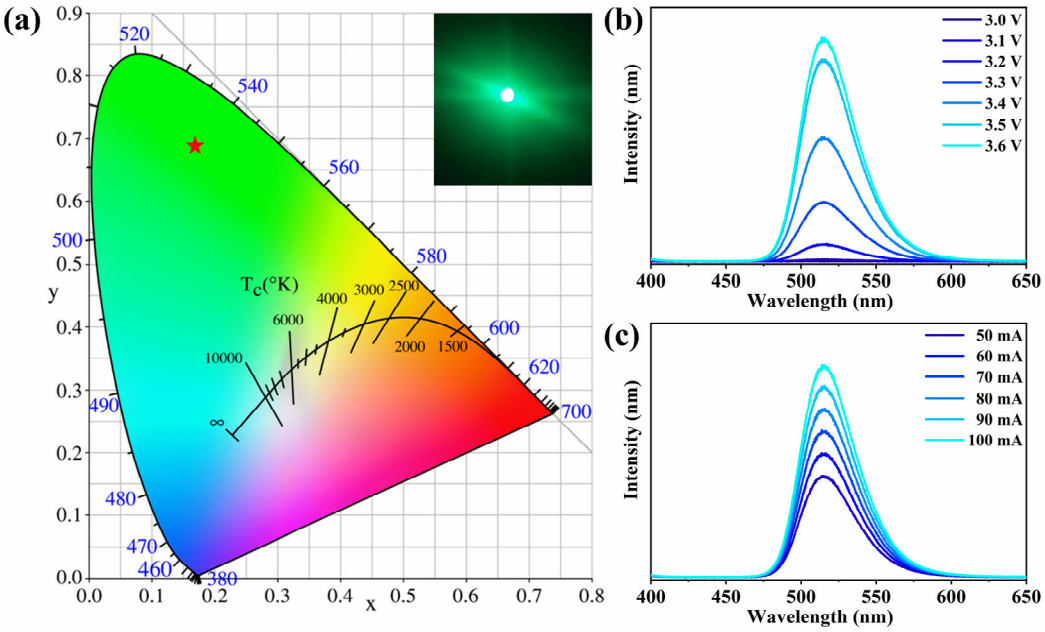

Figure S6. (**a**) The CIE coordinates of the fabricated LED. Emission spectra of the fabricated LED at different driving voltage (**b**) and currents (**c**).

Table S2. The main optoelectronic application directions of typical Mn(II)-based metal halides.

Compound	Emission Wavelength	PLQY	Optoelectronic Application	Ref
$(HTPP)_2MnBr_4$	519 nm	98.6%	X-ray scintillator	[57]
$(MTP)_2MnBr_4$	516 nm	99.5%	X-ray scintillator	[58]
BTP_2MnBr_4	510 nm	91%	X-ray scintillator	[59]
$(ETP)_2MnBr_4$	520 nm	84%	X-ray scintillator	[60]
$(C_5H_6N)_2MnBr_4$	520 nm	59.36%	X-ray scintillator	[61]
Cs_3MnI_5	540 nm	73%	X-ray scintillator	[62]
$[(H_2C{=}CHCH_2)(C_6H_5)_3P]_2MnBr_4$	516 nm	48%	LED	[19]
$(Ph_4P)_2MnBr_4$	516 nm	98%	LED	[28]
$[Ph_3BzP]_2[MnBr_4]$	517 nm	53%	LED	[63]
$(C_9NH_{20})_2MnBr_4$	528 nm	81.08%	Acetone sensor	[21]
$(TPA)_2MnBr_4$	512 nm	89.23%	Ferbam sensor	[21]
$((CH_3)_4N)((C_2H_5)_4N)_2(MnBr_{4-x}Cl_x)_2NH_4$ (x = 0, 2, 3)	x = 0, 510 nm x = 2, 512 nm x = 3, 513 nm	x = 0, 95% x = 2, 97% x = 3, 99%	Photodetector	[40]